A Power-Splitting Relaying Protocol for Wireless Energy Harvesting and Information Processing in NOMA Systems

Huu Q. Tran [1,2,*], *Tien-Tung Nguyen*[2], *Ca V. Phan*[1], *Quoc-Tuan Vien*[3]

[1] *Ho Chi Minh City University of Technology and Education, Vietnam*
[2] *Industrial University of Ho Chi Minh City, Vietnam*
[3] *Middlesex University, United Kingdom*
* *E-mail: huutq.ncs@hcmute.edu.vn*

Abstract: Non-orthogonal multiple access (NOMA) along with cooperative communications have been recognized as promising candidates for the fifth generation (5G) wireless networks and have attracted many researchers. Every networked device however has its own limited power supply. To this extent, this paper investigates a power-splitting relaying (PSR) protocol for wireless energy harvesting and information processing in the NOMA systems to prolong the lifetime of the energy-constrained relay nodes in wireless networks so as to avail the ambient radio-frequency (RF) signal as well as to simultaneously harvest the energy and process the information. Decode-and-forward relaying is employed at the relay node where the energy from the received RF signal is harvested and exploited to forward the information to the destination. Specifically, the outage probability and ergodic rate of the PSR protocol are derived to realize the impacts of energy harvesting time, energy harvesting efficiency, power splitting ratio, source data rate, and the distance between nodes. It is also shown that an increased energy harvesting efficiency results in an enhanced performance and an outperformance in terms of the energy efficiency is achieved with the employment of the NOMA when compared to the conventional orthogonal multiple access. Numerical results are provided to verify the findings.

1 Introduction

Recently, there have been numerous research works on wireless energy harvesting (EH) and information processing [1] - [3]. The EH in the wireless relay and wireless sensor networks is necessary due to the limited power storage of relays and sensor nodes which often rely on external charging mechanisms to maintain their operation [4], [5]. In order to prolong the network lifetime, many EH techniques and cooperative relay protocols have been integrated into the devices. The EH circuits can in fact perform simultaneous wireless information and power transfer (SWIPT) which can be used in the various critical environment such as healthcare, disaster, etc.

In [6], a decode-and-forward (DF) relaying protocol was proposed with the EH function where the relays replenish the energy from the received RF signals. In [7], time-switching (TS) based protocols were developed for wireless-powered relay nodes considering both amplify-and-forward (AF) and DF relaying along with SWIPT and energy accumulation at the relays. In [8]-[9], the authors investigated the PS-based SWIPT and proposed to use SWIPT in a full-duplex relay (FDR) network [8] as well as two relay selection stragies in the two way FDR system to minimize the outage probability [9].

The maximum transmission rate schemes for power-switching relaying (PSR) and time-switching relaying (TSR) protocols in the DF-based relay networks were investigated in [10], where the relay is assumed to have a rechargeable battery with a certain amount of remaining energy to harvest the energy from the received RF signal. In [11], a non-shared power allocation scheme was investigated and its performance was analysed and compared to that of several shared power allocation schemes. The EH with a dual-hop half-duplex (HD) and full-duplex (FD) SWIPT employing both the DF and AF relaying was proposed in [12] for log-normal fading channels. In [13], a joint non-orthogonal multiple access (NOMA) and partial relay selection was proposed to employ the AF relaying for enhancing not only sum rate and user fairness, but also the outage probability with a proper power allocation to users subject to a minimum signal-to-noise ratio (SNR). Also, the NOMA has recently been investigated with different approaches for the 5G networks, such as the works in

[14]-[18]. In [19], both FD and HD transmission modes were considered for an AF-based NOMA system. However, the cooperative NOMA systems in general, require the relay to fully cooperate using its own generated power for helping the source to send data to the destination.

In order to tackle the power supply issue at the relay for cooperative communications, in this paper, we investigate the employment of EH and DF-based NOMA in a SWIPT system. A PSR protocol with a power splitting (PS) receiver architecture is considered. In the PSR protocol, the energy-constrained relay node uses a portion of the received power for EH, while the remaining energy is for information processing. In particular, this paper considers two transmission modes at the energy-constrained relay node, including:

i) *Delay-limited transmission (DLT)*: In this mode, the destination node decodes the received signal block by block.
ii) *Delay-tolerant transmission (DTT)*: In this mode, the destination node can buffer the received information blocks and thus it accepts the delay due to the decoding of the received signal, [*]

The main contributions and features of our work are summarized as follows:

• An HD NOMA scheme is proposed for a SWIPT system to allocate power for two users, among which one is considered as a relay node to perform both EH and DF the received signal. The proposed scheme makes use of a PS receiver architecture which enables both information processing and EH at the relay node.
• The performance of the proposed scheme is analysed in terms of outage probability, throughput and ergodic rate. Specifically, closed-form expressions are derived for the outage probability at both users, while the analytical results of the throughput and ergodic rate are obtained for DLT and DTT modes, respectively. It is shown that, with the NOMA adaptation, an enhanced outage performance

---

[*]*For the DTT mode, [20] can apply for different code lengths.*

is achieved for a considerably increased throughput and ergodic rate when compared to the conventional orthogonal multiple access (OMA).

• The energy efficiency is derived for the proposed HD NOMA systems. Our numerical results show that the NOMA achieves a higher EE performance than the conventional OMA.

We structure the rest of the paper as follows. Section II presents the overall system model of the proposed relay assisted cooperative NOMA and assumptions. Sections III describes in detail the performance analysis of the proposed PSR protocol. Section IV shows the simulation results. Finally, Section V concludes this paper and summarizes the key findings.
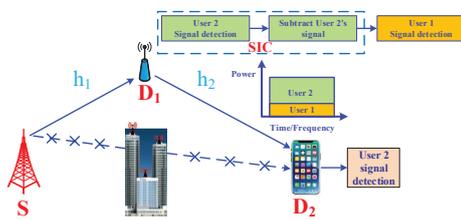
2 SYSTEM MODEL

Fig. 1: System Model.

Figure 1 illustrates the system model under investigation, in which a source node, S, wants to transfer the information to two users D_1 and D_2. It is assumed that there is an obstacle between S and D_2. As shown in Figure 1, S sends data to D_1 and D_1 is exploited to assist the communications from S to D_2. Here, D_1 employs DF relaying protocol using the energy harvested from S. The distances from S to D_1 and from D_1 to D_2 are denoted by d_1 and d_2, respectively. The complex channel coefficients of $S \rightarrow D_1$ and $D_1 \rightarrow D_2$ links are denoted by h_1 and h_2, with respective power gains of $|h_1|^2$ and $|h_2|^2$, which are assumed to be exponentially distributed with $E[|h_1|^2]=\Omega_1^{-1}$ and $E[|h_2|^2]=\Omega_2^{-1}$. Here, E[.] denotes expectation operation.
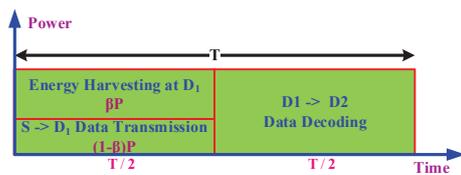
2.1 Energy Harvesting at D_1

Fig. 2: PSR Protocol of Energy harvesting system.

Figure.2 presents the communication block diagram using PSR protocol for EH and information processing at D_1 in the total time block of T. The power of the received signal at D_1 is denoted by P. It is assumed that S transmits information to D_1 in the first half of T, while the remaining time, i.e. $T/2$, is dedicated for transmitting the information from D_1 to D_2.

With the employment of superposition of the transmitted signals at S as in the NOMA scheme, the observation at D_1 is given by

$$y_{D_1} = h_1(\sqrt{a_1 P_s}x_1 + \sqrt{a_2 P_s}x_2) + n_{D_1}, \quad (1)$$

where P_s is transmission power at S, a_1 and a_2 are power allocation coefficients for data symbols x_1 and x_2 that are wished to send from S to D_1 and D_2, respectively, and n_{D_1} is additive white Gaussian noise (AWGN) at D_1 with zero mean and variance σ^2. It is assumed that $E[x_1^2] = E[x_2^2] = 1$, and, without loss of generality, $a_2 > a_1 > 0$ satisfying $a_1 + a_2 = 1$.

Employing PSR protocol, D_1 splits the received power into two parts including: i) harvested energy and ii) information processing energy. Let β, $0 < \beta < 1$, denote the power splitting ratio. The energy harvested at D_1 can be obtained as

$$E_H = \beta\eta|h_1|^2\rho\,(T/2), \quad (2)$$

where $\rho \triangleq P_s/\sigma^2$ represents the transmit signal-to-noise ratio (SNR) and $0 < \eta < 1$ denotes the energy harvesting efficiency at the energy receiver which is dependent of the rectifier and the energy harvesting circuitry. All the energy harvested during energy harvesting phase is consumed at D_1 while forwarding the decoded signal to D_2.

From the harvested energy E_H, the transmission power at D_1 can be given by

$$P_r = \frac{E_H}{(T/2)} = \frac{\beta\eta|h_1|^2\rho\,(T/2)}{(T/2)} = \beta\eta|h_1|^2\rho. \quad (3)$$

2.2 Information Processing at D_1 and D_2

Applying the NOMA principle, D_2 is allocated more power than that for D_1. After receiving the signal from S, D_1 decodes the signal x_2 and decodes its own signal x_1 by employing successive interference cancellation (SIC) [21]. We assume that an ideal setup with perfect SIC is given in our model system, i.e, the level of residual interference is zero.

From (1) the received signal to interference plus noise ratio (SINR) at D_1 to detect x_2 of D_2 is given by

$$\gamma_{2,D_1} = \frac{\psi_I|h_1|^2 a_2\rho}{\psi_I|h_1|^2 a_1\rho + 1}, \quad (4)$$

where $\psi_I = (1 - \beta)$ denotes the information processing coefficient in the PSR protocol. After SIC, there is no interference remaining in the received signal at D_1. The received SNR at D_1 to detect its own message x_1 is thus given by

$$\gamma_{1,D_1} = \psi_I|h_1|^2 a_1\rho. \quad (5)$$

Meanwhile, the decoded signal x_2 at D_1 is forwarded to D_2. The received signal at D_2 can be expressed as

$$y_{D_2} = \left(\sqrt{P_r}x_2\right)h_2 + n_{D_2}. \quad (6)$$

Substituting Eq. (3) into y_{D_2}, we obtain

$$y_{D_2} = \left(\sqrt{\beta\eta\rho}\right)|h_1|\,h_2 x_2 + n_{D_2}. \quad (7)$$

The received SNR at D_2 is thus given by

$$\gamma_{2,D_2} = |h_2|^2|h_1|^2\psi_E\rho, \quad (8)$$

where $\psi_E = \beta\eta$ denotes the energy harvesting coefficient in the PSR protocol.

2

3 PERFORMANCE ANALYSIS

3.1 Outage Performance

3.1.1 Outage Probability at D_1:
In the NOMA protocol, D_1 is not in outage when it can decode both x_1 and x_2 received from S. Therefore, the outage probability at D_1 can be expressed by

$$P_{D_1,PSR}^{HD} = 1 - \text{Pr}\left(\gamma_{2,D_1} > \gamma_{th_2}^{HD}, \gamma_{1,D_1} > \gamma_{th_1}^{HD}\right), \quad (9)$$

where $\gamma_{th_1}^{HD} = 2^{2R_1} - 1$ and $\gamma_{th_2}^{HD} = 2^{2R_2} - 1$. Here, R_1 and R_2 are the target rates for detecting x_1 and x_2 at D_1, respectively. We have the following finding of the outage probability at D_1.

Theorem 1. *The outage probability at D_1 is given by*

$$P_{D1,PSR}^{HD} = 1 - e^{-\frac{\theta_1}{\Omega_1}}, \quad (10)$$

where $\theta_1 = \max(\tau_1, \nu_1), \tau_1 = \frac{\gamma_{th2}^{HD}}{\rho\psi_I(a_2 - a_1\gamma_{th2}^{HD})}$ and $\nu_1 = \frac{\gamma_{th1}^{HD}}{a_1\psi_I\rho}$ with $a_2 > a_1\gamma_{th2}^{HD}$.

Proof: The outage probability at D_1 can be computed by

$$P_{D_1,PSR}^{HD} = 1 - P_r\left(|h_1|^2 \geq \theta_1\right)$$

$$= 1 - \int_{\theta_1}^{\infty} f_{|h_1|^2}(y)\, dy \quad (11)$$

$$= 1 - e^{-\frac{\theta_1}{\Omega_1}}.$$

The proof is completed. □

3.1.2 Outage Probability at D_2:
Note that the far-end node D_2 is in outage when either D_1 can not detect x_2 or D_2 can not recover the forwarded signal from D_1. The outage probability at D_2 can be derived as (see (12)). Deriving J_2 and J_3, we have the following finding

Theorem 2. *The outage probability at D_2 can be given by*

$$P_{D_2,PSR}^{HD} = 1 - e^{-\frac{\tau_1}{\Omega_1}} +$$

$$\int_{\tau_1}^{\infty}\left(1 - e^{-\frac{\gamma_{th2}^{HD}}{x\psi_E\rho\Omega_2}}\right)\frac{1}{\Omega_1}\exp\left(\frac{-x}{\Omega_1}\right)dx. \quad (13)$$

Proof: Considering Rayleigh fading channel, J_2 (see (12)) can be given by

$$J_2 = 1 - \exp\left(\frac{-\tau_1}{\Omega_1}\right). \quad (14)$$

and J_3 can be expressed as (see (15)). The outage probability at D_2 is thus given by

$$P_{D_2,PSR}^{HD} = J_2 + J_3 \quad (16)$$

□

Corollary 1. *In the case of high SNR, the outage probability at D_2 can be derived as (see (17)), where $K_1(.)$ denote the first order modified Bessel function of the second kind [22, Eq.(9.6.22)].*

3.2 Throughput for Delay-limited Transmission Mode

In this mode, it is assumed that the source node transmits information with a constant rate of R, depending on the performance of the outage probability due to wireless fading channels. The system

throughput of HD transmission mode in the NOMA system is thus given by

$$\tau_{t,PSR}^{HD} = \left(1 - P_{D_1,PSR}^{HD}\right)R_1 + \left(1 - P_{D_2,PSR}^{HD}\right)R_2, \quad (18)$$

where $P_{D_1,PSR}^{HD}$ and $P_{D_2,PSR}^{HD}$ can be obtained from (10) and (16), respectively.

3.3 Ergodic Rate for Delay-tolerant Transmission Mode

3.3.1 Ergodic Rate at D_1:
For the case when D_1 can detect x_2, the achievable rate at D_1 can be written as

$$R_{D_1,PSR}^{HD} = \frac{1}{2}\log_2\left(1 + \gamma_{1,D_1}\right). \quad (19)$$

The ergodic rate at D_1 for HD transmission mode in the NOMA system can be obtained by the following theorem.

Theorem 3. *The ergodic rate at D_1 is given by*

$$R_{D_1,PSR}^{HD} = \frac{-\exp\left(\frac{1}{\psi_I a_1\rho\Omega_1}\right)}{2\ln 2}Ei\left(\frac{-1}{\psi_I a_1\rho\Omega_1}\right). \quad (20)$$

$Ei(x)$ denotes the exponential integral function [23, Eq.(3.352.4)].

Proof: See Appendix 1.

□

3.3.2 Ergodic Rate at D_2:
Since x_2 needs to be detected at both D_1 and D_2, the achievable rate at D_2 for HD transmission mode in the NOMA system can be written as

$$R_{D_2,PSR}^{HD} = \frac{1}{2}\log_2\left(1 + \min\left(\gamma_{2,D_1}, \gamma_{2,D_2}\right)\right). \quad (21)$$

Theorem 4. *The ergodic rate at D_2 is given by*

$$R_{D_2,PSR}^{HD} = \frac{1}{2\ln 2}\int_0^{\frac{a_2}{a_1}}\left[\frac{e^{-\frac{x}{\psi_I\rho(a_2 - a_1x)\Omega_1}}}{1+x}\right.$$

$$\left. + \frac{\int_{\frac{x}{\psi_I\rho(a_2-a_1x)}}^{\infty}\frac{x}{\Omega_1}\left(1 - e^{-\frac{x}{y\rho\psi_E\Omega_2}}\right)e^{-\frac{y}{\Omega_1}}dy}{1+x}\right]dx. \quad (22)$$

Proof: See Appendix 2. □

Remark 1. *Thus the corresponding ergodic rate is given by*

$$R_{D_2,PSR}^{HD,\infty} = \frac{1}{2\ln 2}\int_0^{\infty}\frac{1 - F_X(x)}{1+x}dx. \quad (23)$$

From the analytical result in (23), for the high SNR region $\rho \to \infty$, the asymptotic expression for the ergodic rate at D_2 can be given by

$$R_{D_2,PSR}^{HD,\infty} = \frac{1}{2\ln 2}\int_0^{\frac{a_2}{a_1}}\frac{2\sqrt{\frac{x}{\psi_E\rho\Omega_1\Omega_2}}K_1\left(2\sqrt{\frac{x}{\psi_E\rho\Omega_1\Omega_2}}\right)}{1+x}dx. \quad (24)$$

.

Proof: See Appendix 3. □

.

3

$$P_{D_2,PSR}^{HD} = \underbrace{\Pr\left(\gamma_{2,D_1} < \gamma_{th_2}^{HD}\right)}_{J_2} + \underbrace{\Pr\left(\gamma_{2,D_2} < \gamma_{th_2}^{HD}, \gamma_{2,D_1} > \gamma_{th_2}^{HD}\right)}_{J_3}. \tag{12}$$

$$J_3 = \Pr\left(|h_2|^2|h_1|^2\psi_E\rho < \gamma_{th_2}^{HD}, \frac{|h_1|^2\psi_I a_2\rho}{\psi_I|h_1|^2 a_1\rho+1} > \gamma_{th_2}^{HD}\right) = \begin{cases} \Pr\left(|h_2|^2 < \frac{\gamma_{th_2}^{HD}}{|h_1|^2\psi_E\rho}, |h_1|^2 > \frac{\gamma_{th_2}^{HD}}{\psi_I\rho\left(a_2-a_1\gamma_{th_2}^{HD}\right)}\right), a_2 > a_1\gamma_{th_2}^{HD} \\ \\ 0, \ a_2 \le a_1\gamma_{th_2}^{HD} \end{cases}$$

$$= \int\limits_{\frac{\gamma_{th_2}^{HD}}{\psi_I\rho\left(a_2-a_1\gamma_{th_2}^{HD}\right)}}^{\infty} \int\limits_{0}^{\frac{\gamma_{th_2}^{HD}}{x\psi_E\rho}} f_{|h_1|^2}(x)f_{|h_2|^2}(y)dxdy = \int\limits_{\tau_1}^{\infty} \frac{1}{\Omega_{1,PSR}}\left[1-\exp\left(\frac{-\gamma_{th_2}^{HD}}{x\psi_E\rho\Omega_{2,PSR}}\right)\right]\exp\left(\frac{-x}{\Omega_{1,PSR}}\right)dx. \tag{15}$$

$$P_{D_2,PSR}^{HD,\infty} = \Pr\left(\frac{a_2}{a_1} < \gamma_{th_2}^{HD}\right) + \Pr\left(|h_2|^2 < \frac{\gamma_{th_2}^{HD}}{\psi_E\rho|h_1|^2}, \frac{a_2}{a_1} > \gamma_{th_2}^{HD}\right)$$

$$= \Pr\left(|h_2|^2 < \frac{\gamma_{th_2}^{HD}}{\psi_E\rho|h_1|^2}, \frac{a_2}{a_1} > \gamma_{th_2}^{HD}\right) = \int\limits_0^\infty \left[1-\exp\left(\frac{-\gamma_{th_2}^{HD}}{\psi_E\rho\Omega_2 x}\right)\right]\frac{1}{\Omega_1}\exp\left(\frac{-x}{\Omega_1}\right)dx = 1 - 2\sqrt{\frac{\gamma_{th_2}^{HD}}{\psi_E\rho\Omega_1\Omega_2}}K_1\left(2\sqrt{\frac{\gamma_{th_2}^{HD}}{\psi_E\rho\Omega_1\Omega_2}}\right). \tag{17}$$

3.3.3 Ergodic rate of the system:
The system ergodic rate of HD transmission mode in the NOMA system is thus given by

$$\tau_{r,PSR}^{HD} = R_{D_1,PSR}^{HD} + R_{D_2,PSR}^{HD}, \tag{25}$$

where $R_{D_1,PSR}^{HD}$ and $R_{D_2,PSR}^{HD}$ can be obtained from (20) and (22), respectively.

3.4 Imperfect SIC

Considering the imperfect SIC symbol x_2 received at D_1.

The observation at D_1 is given by [24]

$$\hat{y}_{D_1} = h_1\left(\sqrt{a_1 P_S}x_1 + \kappa\sqrt{a_2 P_S}x_2\right) + n_{D_1}, \tag{26}$$

where κ, $0 \le \kappa \le 1$, denotes the level of residual interference due to the imperfect SIC at D_1 [25]. Specifically, $\kappa = 0$ and $\kappa = 1$ refer to the cases of perfect SIC and fully imperfect SIC, respectively. According to theory, the κ value can vary from 0 to 1 depending on SIC efficiency. For NOMA, one usually assume that the problem is solved with perfect SIC, i.e. $\kappa = 0$. Thus, the effectiveness of the NOMA is better than OMA. For the case of imperfect SIC, a small change of the SIC residual interferene, e.g. $\kappa = 0.15$, also considerably affects on the performance of NOMA system. Even, this causes a worse performance as compared to the conventional OMA. Thereby, a SIC design is the key issue in NOMA technique.

The SINR at D_1 to detect x_1 is given by

$$\overset{\wedge}{\gamma}_{1,D_1} = \frac{\psi_I|h_1|^2 a_1\rho}{\psi_I|h_1|^2\kappa^2 a_2\rho + 1}. \tag{27}$$

From (27), the outage probability of detecting x_1 with imperfect SIC at D_1 can be expressed as

$$P_{x_1,D_1}^{I\_SIC} = \Pr\left[\left(\frac{\psi_I|h_1|^2 a_1\rho}{\psi_I|h_1|^2\kappa^2 a_2\rho+1}\right) < \gamma_{th_1}\right]$$

$$= 1 - \Pr\left[\left(\frac{\psi_I|h_1|^2 a_1\rho}{\psi_I|h_1|^2\kappa^2 a_2\rho+1}\right) \ge \gamma_{th_1}\right]$$

$$= 1 - \Pr\left(|h_1|^2 \ge \overset{\wedge}{\theta}_1\right),$$

where

$$\Pr\left(|h_1|^2 \ge \overset{\wedge}{\theta}_1\right) = \int\limits_{\overset{\wedge}{\theta}_1}^{\infty} f_{|h_1|^2}(y)dy$$

Then

$$P_{x_1,D_1}^{I\_SIC} = 1 - \int\limits_{\overset{\wedge}{\theta}_1}^{\infty} f_{|h_1|^2}(y)dy = 1 - e^{-\frac{\overset{\wedge}{\theta}_1}{\Omega_1}}, \tag{28}$$

where $\overset{\wedge}{\theta}_1 = \frac{\gamma_{th_1}}{\rho\psi_I\left(a_1 - a_2\kappa^2\gamma_{th_1}\right)}$.

3.5 Energy efficiency

From throughput and ergodic rate analysis results, we aim to provide energy efficiency (EE) considering user relaying for HD NOMA systems. The EE is defined as the ratio of the total achievable data rate and the total power consumption in the whole network, which is given by EE $\overset{\Delta}{=} \frac{R}{P_s+P_r}$, where R denotes the total network throughput, P_s is the power transmission at the source, and P_r is the power transmission at the relay (see (3)). The energy efficiency of user

4

relaying for HD NOMA systems can be expressed as

$$EE_\phi = \frac{2\tau_\phi^{HD}}{\rho \left(1 + \psi_E \Omega_1\right)}, \tag{29}$$

where $\phi \in (t, r)$.

4 SIMULATION RESULTS

This section verifies the derived analytical results presented in the preceding sections. The distance between S and D_2 is normalized to unity, i.e. $\Omega_{SD_2} = 1$, $\Omega_{SD_1} = d^{-m}$ and $\Omega_{D_1D_2} = (1-d)^{-m}$, where d is the normalized distance between the S and D_1 and m is the pathloss exponent. It is assumed that $d = 0.3$ and $m = 2$. The power allocation coefficients for D_1 and D_2 are set as $a_1 = 0.2$ and $a_2 = 0.8$, respectively. The target rates are set as $R_1 = 3$ bps and $R_2 = 0.5$ bps.

In the simulation, the performance of the conventional OMA is used as a benchmark for comparison. Specifically, in the OMA scheme, it needs three time slots to send the information from S to D_2. In the first time slot, S sends the message x_1 to user relay D_1. In the second time slot, S sends the message x_2 to D_1. In the third time slot, D_1 decodes and forwards the message x_2 to D_2. In particular, in time slot 1, when S sends the information to D_1, there is only x_1 term, thus the outage probability is determined without interference and the message x_2. This can be explained for fair comparison to NOMA in term of power as follows. The power must be decreased a half at $a_1 = 0.5$, $a_2 = 0$ at the first time slot and $a_1 = 0$, $a_1 = 0.5$ at the sending time slot of x_2 (the second time slot), obviously. In the third time slot, D_1 decodes and forwards the message x_2 to D_2. Therefore, the throughput and the ergodic of OMA are equal $1/3$ times of the one of NOMA.

The first work we consider is the evaluation of the outage probability of the system. Figs. 3-6 illustrate the outage probability of two users for the PSR protocol versus SNR and β, respectively. It can be observed that User 2 obtains a lower outage probability than that of User 1 in the HD NOMA scheme as well as in the HD OMA scheme. Also, the outage probability of two users in the HD NOMA scheme is shown to be lower than those in the HD OMA scheme.

In Figs. 3 and 4, with $\beta = 0.6$, $\eta = 0.8$, $d = 0.3$, $m = 2$, $a_1 = 0.2$, $a_2 = 0.8$, $a_{1\_OMA} = 0.5$ and $a_{2\_OMA} = 0.5$, the outage probabilities of the PSR protocol are as a function of SNR (dB) where the User1-exact is significantly higher than the User2-exact.
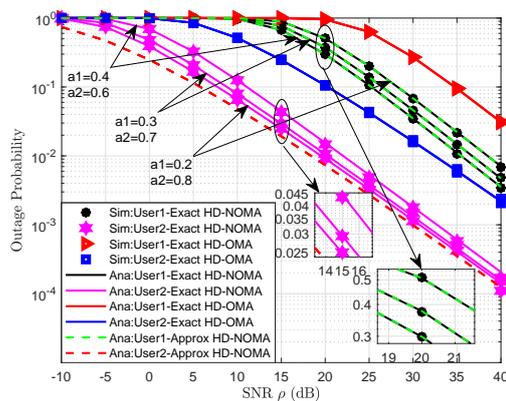

Fig. 3: Outage probability of two users for the PSR protocol versus transmitting SNR and different coefficients of a_1, a_2.

For example, the User1-exact has a higher outage probability than that of the User2-exact about 36% at $SNR = 20(dB)$ in the HD NOMA scheme. The PSR protocol achieves better performance when SNR increases. These results can be explained as follows. When SNR increases, the harvested energy E_H in (2) and received SNRs γ_{2,D_1} and γ_{1,D_1} in (4) and (5) at D_1 increase in the PSR protocol, respectively.
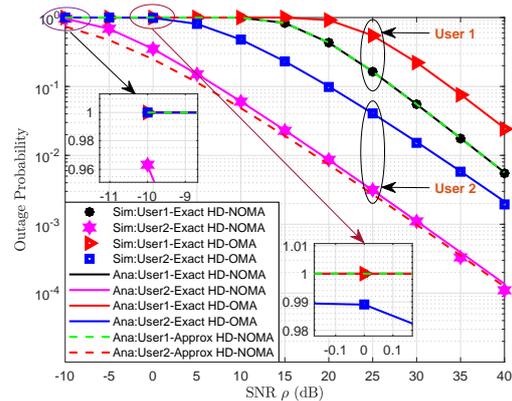

Fig. 4: Outage probability of two users for the PSR protocol versus transmitting SNR.

In Fig. 5, the outage probability of the PSR protocol as a function of the β on the x-axis is set from 0.001 to 1 with 0.08 step.
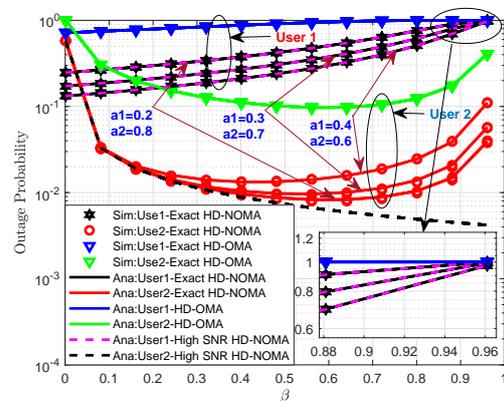

Fig. 5: Outage probability of two users for the PSR protocol versus β and different coefficients of a_1, a_2.

For instance, with $\eta = 0.8$, $d = 0.3$, $m = 2$, $a_1 = 0.2$, $a_2 = 0.8$, $a_{1\_OMA} = 0.5$ and $a_{2\_OMA} = 0.5$, as shown in Fig. 6, the exact theoretical curves for the outage probability of two users for HD NOMA are plotted according to (9), (10), (12), (13) and (17), respectively. The curve representing the outage probability of User 1 gradually increases according to β in (10) while that of User 2 decreases in range of β of about 0 to 0.6 and then rapidly changes but not be linear in case of β of from 0.6 to 1. This change is caused by the parameters containing in (13). Resulting in that these curves intersect each other at some points in the figure. Furthermore, it can be explained based on the equations that the more ρ increases,

5

the more τ_1 decreases. The curves of Analytical-User1-Exact HD-NOMA and Analytical-User1-High SNR HD-NOMA are overlap each other. The curve representing of Analytical-User2-Exact HD-NOMA is plotted based on (13) while Analytical-User2-High SNR HD-NOMA is based on (17). It can be observed that the red curve is parallel and approximate with the black dashed curve in range of ρ from 0 to 0.2. Then, Analytical-User2-High SNR HD-NOMA raplidly decreases when ρ increasingly varies as shown in Fig. 6. These explanation can be also employed for Fig. 5 where the simulation scenario of the outage probability is simulated with different coefficients of a_1, a_2. The exact outage probability curves precisely also match with the Monte Carlo simulation results.
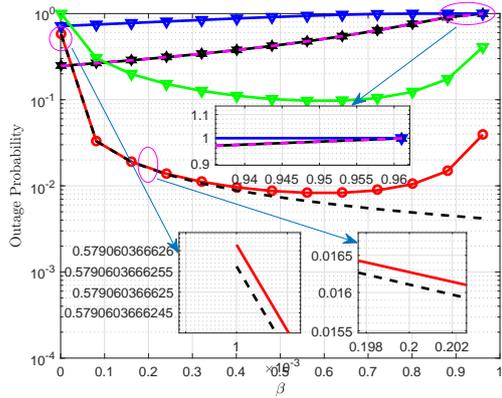
Fig. 6: Outage probability of two users for the PSR protocol versus β.

Figure 7 plots the comparison of the outage probabilities at D_1 versus SNR corresponding with imperfect and perfect SIC symbol x_2 with different values of κ. As shown in Fig. 7, the SIC residual interference coefficient has a considerable impact on the outage performance at D_1. It is noticed that in range of κ of from 0 to 1, the smaller the κ value, the better the SIC and the smaller the residual interference, and vice versa.
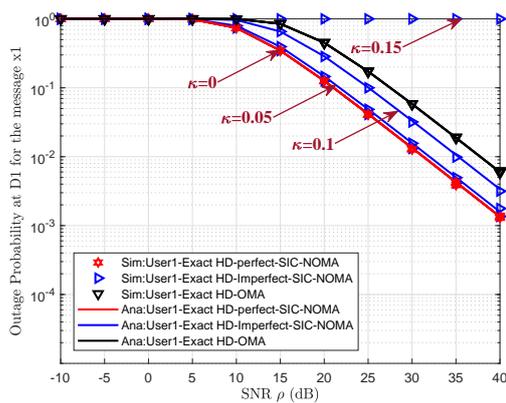

Fig. 7: Comparison of the outage probability at D_1 versus transmitting SNR for the cases of perfect and imperfect SIC x_2 with different values of κ.

As aslo shown in Fig. 7, the outage probability tends to increase as the k becomes higher. It can be observed that when κ is large enough, i.e. $\kappa > 0.15$ as shown in the figure, the outage probability is approximately equal 1 in the SNR region of from -10 to 40 dB.

Considering the system throughput for DLT mode and ergodic rate for DTT mode, Figs. 8-10 sequentially plot throughput and ergodic rate of two users for the PSR protocol as a function of the β, $\eta = 0.8$, $d = 0.3$, $m = 2$, $a_1 = 0.2$, $a_2 = 0.8$, $a_{1\_OMA} = 0.5$ and $a_{2\_OMA} = 0.5$. Specifically, it can be seen in Fig. 8 that the throughput of User 1 is significantly higher than that of User 2 in the HD NOMA scheme. In contrary, the throughput of User 1 is lower than that of User 2 in the HD OMA scheme. This is due to the fact that D_1 receives both x_1 and x_2 signals while D_2 receives only x_2 in the DLT mode.
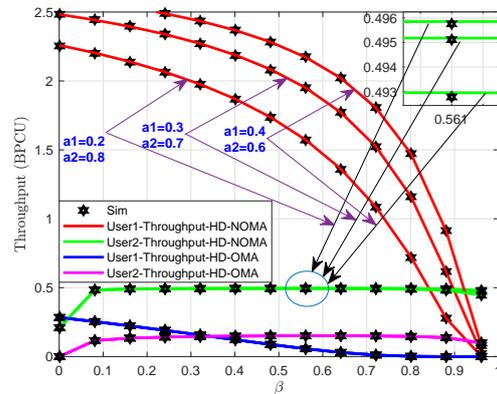

Fig. 8: The throughput of two users for the PSR protocol versus β and different coefficients of a_1, a_2.

A similar observation can be realised in Figs. 9 and 10 where the ergodic rate at User 1 is higher than that in both the HD NOMA and the HD OMA schemes.
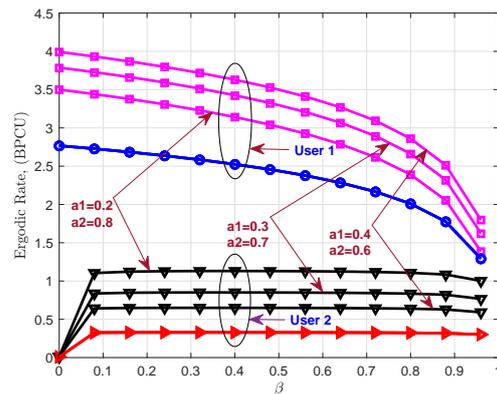

Fig. 9: The ergodic rate of two users for the PSR protocol versus β and different coefficients of a_1, a_2.

The ergodic rate at User 1 is shown to be the highest, while the one at User 2 is the lowest in the HD OMA scheme. This can be explained that the SNR at D_1 used to detect x_1 and x_2 in (19) and

6

(20) is higher than the minimum value of SNR at D_1 used to detect x_2 and SNR at D_2 used to detect x_2 in (21) and (22), respectively.
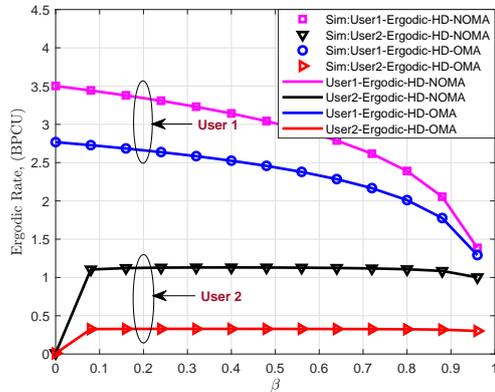

Fig. 10: The ergodic rate of two users for the PSR protocol versus β.

Figure 11 plots the energy efficiency of two users for the PSR protocol as a function of SNR (dB) with $\beta = 0.3$, $\eta = 0.8$, $d = 0.3$, $m = 2$, $a_1 = 0.2$, $a_2 = 0.8$, $a_{1\_OMA} = 0.5$ and $a_{2\_OMA} = 0.5$. It shows that EE performance in the DLT mode is lower than that in the DTT mode. Thus, NOMA has outperformed EE performance compared with conventional OMA in low SNR region (SNR < 10 (dB)). The reason is that HD NOMA can achieve larger throughput and ergodic rate than that of HD OMA. The exact theoretical curves for the ergodic rate of two users for HD NOMA are plotted according to (29). About explanation for inflection points, when the value of SNR is in lower range, EE decreases rapidly. However, the graph of EE varies towards gradually decreasing as SNR value is towards increasing according to (29). These lead to existing inflection points in the simulation result figure.
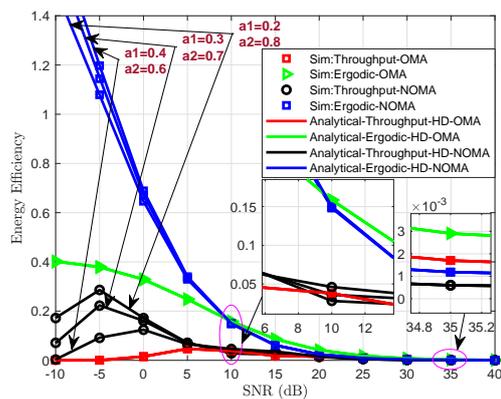

Fig. 11: Energy efficiency of two users for the PSR protocol and different coefficients of a_1, a_2.

Moreover, it can be seen in Fig. 11 as well as in (29) that EE versus throughput for DLT mode changes quickly according to the follow function $F(1/exp)$ (see (18)) with $a_1 = 0.2$, $a_2 = 0.8$ while the EE of OMA system varies according to function

$F(1/exp)$ with $a_{1\_OMA} = 0.5$, $a_{2\_OMA} = 0.5$. For instance, the intersection of the curves of Analytical-Thoughput-HD-NOMA and Analytical-Thoughput-HD-OMA at $SNR = 8.55562295\,(dB)$ yields the cutting points as shown in Fig. 12.
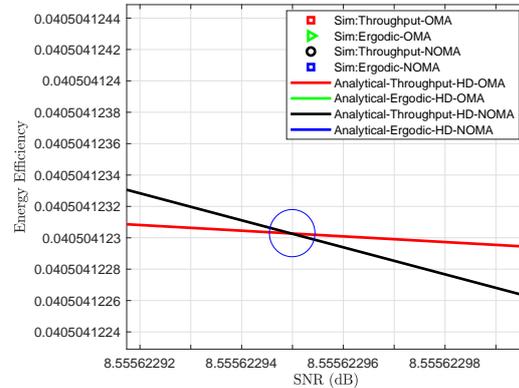

Fig. 12: Energy efficiency of two users for the PSR protocol.

Besides, based on (25), we can explained that EE versus ergodic rate for DTT mode of NOMA system decreases more and more according to the follow function $F(1/(2\ln 2))$ while that of OMA system varies slowly according to function $F(1/(3\ln 2))$. As a result, there occur the intersectons at some points as well as inflection points among the curves as shown in Figs. 11 and 13. For example, as plotted in Fig. 13, it can be observed that the curves of Analytical-Ergodic-HD-NOMA also intersect that of Analytical-Ergodic-HD-OMA at $SNR = 9.4261806\,(dB)$.
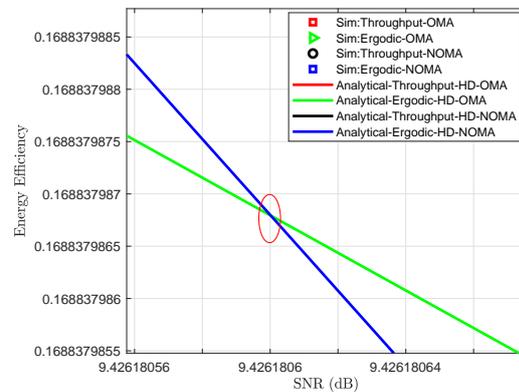

Fig. 13: Energy efficiency of two users for the PSR protocol.

Figs. 14 and 15 clearly illustrate the non-intersection of the curves as asymptotically decreasing to 0 with SNR in region of from 25 to 40 dB.
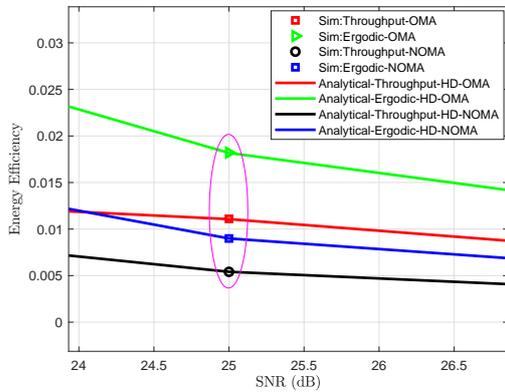
7

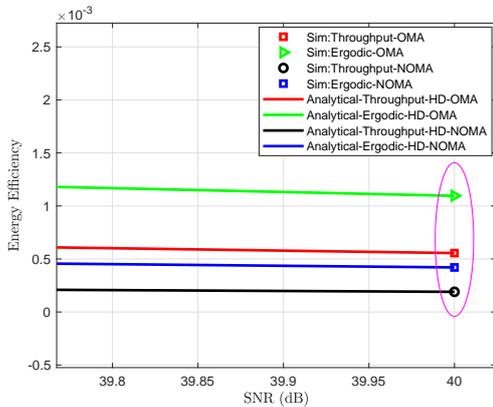**Fig. 14**: Energy efficiency of two users for the PSR protocol.

Fig. 15: Energy efficiency of two users for the PSR protocol.

Therefore, we can conclude that the simulation results in Figs. 4-15 match analytic results mentioned in above sections.

5 CONCLUSION

In this paper, an EH scheme has been proposed along with the adaptation of NOMA for a SWIPT system. A PSR has been employed for the DF relaying protocol. The closed-form expressions of outage probability at two users have been derived along with the expressions of the achievable throughput, ergodic sum rate and EE. Numerical results have shown that NOMA outperformed the conventional OMA in terms of both throughput and ergodic rate. It has also shown that the NOMA achieves a lower outage probability at the far-end user and a better EE performance in the low-SNR regime compared to the conventional OMA.

For future work, we will investigate the performance of the proposed PSR for EH in cooperative NOMA taking into account the impacts of the direct link between source and far-end user.

6 References

1 R. Zhang and C. K. Ho.: 'MIMO broadcasting for simultaneous wireless information and power transfer', *IEEE Transactions on Wireless Communications*, 2013, 12, (5), pp. 1989-2001

2 P. Popovski, A. M. Fouladgar, and O. Simeone.: 'Interactive joint transfer of energy and information', *ArXiv Technical Report*, 2012

3 Z. Xiang and M. Tao.: 'Robust beamforming for wireless information and power transmission', *IEEE Wireless Communications Letters*, 2012, 1, (4), pp. 372-375

4 P. T. Venkata, S. N. A. U. Nambi, R. V. Prasad, and I. Niemegeers.: 'Bond graph modeling for energy-harvesting wireless sensor networks', *IEEE Computer Society*, Sep 2012, 45, (9), pp. 31-38

5 B. Medepally and N. B. Mehta.: 'Voluntary energy harvesting relays and selection in cooperative wireless networks', *IEEE Trans. Wireless Commun.*, Nov. 2010, 9, (11), pp. 3543-3553

6 Yanju Gu; Sonia Assa.: 'RF-based Energy Harvesting in Decode-and-Forward Relaying Systems: Ergodic and Outage Capacities', *IEEE Transactions on Wireless Communications*, 2015, 14, (11), pp. 6425-6434

7 Ali A. Nasir, Xiangyun Zhou, Salman Durrani, Rodney A. Kennedy.: 'Wireless-Powered Relays in Cooperative Communications: Time-Switching Relaying Protocols and Throughput Analysis', *IEEE Transactions on Communications*, 2015, 63, (5), pp. 1607-1622

8 Dexin Wang; Rongqing Zhang ; Xiang Cheng ; Liuqing Yang, 'Capacity-Enhancing Full-Duplex Relay Networks based on Power Splitting (PS-)SWIPT', *IEEE Transactions on Vehicular Technology*, 2017, 66, (6), pp. 5445-5450

9 Dexin Wang; Rongqing Zhang; Xiang Cheng; Liuqing Yang; Chen Chen, 'Relay Selection in Full-Duplex Energy-Harvesting Two-Way Relay Networks', *IEEE Access*, 2017, 1, (2), pp. 182-191

10 MinChul Ju; Kyu-Min Kang ; Kyu-Sung Hwang ; Cheol Jeong, 'Maximum Transmission Rate of PSR/TSR Protocols in Wireless Energy Harvesting DF-Based Relay Networks', *IEEE Journal on Selected Areas in Communications*, 2015, 33, (12), pp. 2701-2717

11 Lina Elmorshedy; Cyril Leung.: 'Power Allocation in an RF Energy Harvesting DF Relay Network in the Presence of an Interferer', *IEEE Access*, 2017, 5, pp. 7606-7618

12 Khaled Maaiuf Rabie, Bamidele Adebisi, Mohamed-Slim Alouini.: 'Half-Duplex and Full-Duplex AF and DF Relaying With Energy-Harvesting in Log-Normal Fading', *IEEE Transactions on Green Communications and Networking*, 2017, 1, (4), pp. 468-480

13 S. Lee, D. B. da Costa, Q.-T. Vien, T. Q. Duong, and R. T. de Sousa Jr.: 'Non-orthogonal multiple access schemes with partial relay selection', *IET Communications*, 2017, 11, (6), pp. 846-854

14 H. Q. Tran, P. Q. Truong, C. V. Phan, and Q.-T. Vien.: 'On the energy efficiency of NOMA for wireless backhaul in multi-tier heterogeneous CRAN', *in Proc. SigTelCom*, Da Nang, Vietnam, January 2017, pp. 229-234

15 Q.-T. Vien, T. A. Le, C. V. Phan, and M. O. Agyeman.: 'An energy-efficient NOMA for small cells in heterogeneous CRAN under QoS constraints', *in Proceedings European Wireless Conference (EW 2017)*, Dresden, Germany, May 2017, pp. 80-85

16 Q.-T. Vien, T. A. Le, B. Barn and C. V. Phan.: 'Optimising energy efficiency of non-orthogonal multiple access for wireless backhaul in heterogeneous cloud radio access network', *IET Communications*, 2016, 10, (18), pp. 2516-2524

17 N. Bhuvanasundaram, H. X. Nguyen, R. Trestian, and Q.-T. Vien.: 'Non-orthogonal multiple access schemes for next-generation 5G networks: A survey. In: 5G Radio Access Networks: Centralized RAN, Cloud-RAN and Virtualization of Small Cells', *CRC Press*, 2017, pp. 51-66

18 H. Q. Tran, C. V. Phan, and Q.-T. Vien.: 'An overview of 5G technologies. In: Emerging Wireless Communication & Network Technologies: Principle, Paradigm and Performance', *Springer*, 2018, pp. 59-80

19 Xinwei Yue, Yuanwei Liu, Shaoli Kang, Arumugam Nallanathan, and Zhiguo Ding.: 'Exploiting Full/Half-Duplex user relaying in NOMA systems', *IEEE Computer Society*, 2018, 66, (2), pp. 560-575

20 L. Liu, R. Zhang, and K.-C. Chua.: 'Wireless information transfer with opportunistic energy harvesting', *IEEE Transactions on Wireless Communications*, 2013, 12, (1), pp. 288-300

21 S. Luo, R. Zhang, and T. J. Lim.: 'Optimal save-then-transmit protocol for energy harvesting wireless transmitters', *IEEE Transactions on Wireless Communications*, 2013, 13, (3), pp. 1196-1207

22 Abramowitz, M., Stegun, I.A.: 'Handbook of mathematical functions with formulas, graphs, and mathematical tables'(Dover, New York, 1972)

23 Gradshteyn, I.S., Ryzhik, I.M.: 'Table of integrals, series and products' (Academic, San Diego, CA, 2000, 6th edn.)

24 Mahady, Islam Abu, Ebrahim Bedeer, Salama Ikki, and Halim Yanikomeroglu.: 'Sum-Rate Maximization of NOMA Systems under Imperfect Successive Interference Cancellation', *IEEE Communications Letters*, March 2019, 23, (3), pp. 474 - 477

25 Yue, Xinwei, Zhijin Qin, Yuanwei Liu, Shaoli Kang, and Yue Chen.: 'A unified framework for non-orthogonal multiple access', *IEEE Transactions on Communications*, May 2018, 66, (11), pp. 5346-5359

7 Appendices

7.1 Appendix 1 - Proof of Theorem 1

In this appendix, we present the proof of (20). To obtain this closed-form expression, the ergodic rate of D_1 for HD NOMA can be

written as

$$R_{D_1,PSR}^{HD} = \frac{1}{2}E\left[\log_2\left(1 + \psi_I|h_1|^2 a_1\rho\right)\right]$$

$$= \frac{1}{2\ln 2}\int_0^\infty \frac{1 - F_X(x)}{1+x}dx, \qquad (30)$$

The cumulative distribution function (CDF) of X is calculated as follows

$$F_X(x) = \Pr\left(|h_1|^2 < \frac{x}{\psi_I a_1\rho}\right)$$

$$= \int_0^{\frac{x(z\rho+1)}{\psi_I a_1\rho}} \frac{1}{\Omega_1}e^{-\frac{y}{\Omega_1}}dy$$

$$= 1 - e^{-\frac{x}{\psi_I a_1\rho\Omega_1}}, \qquad (31)$$

By replacing (30) in (31), the ergodic rate of D_1 can be derived as

$$R_{D_1,PSR}^{HD} = \frac{1}{2}\frac{1}{\ln 2}\int_0^\infty \frac{1}{1+x}e^{-\frac{x}{\psi_I a_1\rho\Omega_1}}dx$$

$$= \frac{-\exp\left(\frac{1}{\psi_I a_1\rho\Omega_1}\right)}{2\ln 2}Ei\left(\frac{-1}{\psi_I a_1\rho\Omega_1}\right)$$

We can derive (20). The proof is completed.

7.2 Appendix 2 - Proof of Theorem 2

In this appendix, the proof begins by giving the ergodic rate of D_2 as follows

$$R_{D_2,PSR}^{HD} = E\left[\frac{1}{2}\log_2\left(1 + \underbrace{\min\left(\gamma_{2,D_1}, \gamma_{2,D_2}\right)}_{J_1}\right)\right]$$

$$J_1 = \underbrace{\min\left(\frac{\psi_I|h_1|^2 a_2\rho}{\psi_I|h_1|^2 a_1\rho + 1}, |h_2|^2|h_1|^2\psi_E\rho\right)}_{X}$$

The CDF of X is calculated as follows (see (32))

I_3 and I_4 are thus given by (see (33)) and (see (34))

And I_{41} and I_{42} are calculated as follows

$$I_{41} = \int_0^\infty \int_0^{\frac{x}{\psi_I\rho(a_2-a_1x)}} \int_0^{\frac{\psi_I a_2}{(\psi_I ya_1\rho+1)\psi_E}} f_{|h_1|^2}(y)f_{|h_2|^2}(z)\,dydz$$

$$= \int_0^{\frac{x}{\psi_I\rho(a_2-a_1x)}} \frac{1}{\Omega_1}\left(1 - e^{-\frac{\psi_I a_2}{(\psi_I ya_1\rho+1)\psi_E\Omega_2}}\right)e^{-\frac{y}{\Omega_1}}dy, (35)$$

And

$$I_{42} = \int_{\frac{x}{\psi_I\rho(a_2-a_1x)}}^\infty \int_0^{\frac{x}{y\psi_E\rho}} f_{|h_1|^2}(y)f_{|h_2|^2}(z)\,dydz$$

$$= \int_{\frac{x}{\psi_I\rho(a_2-a_1x)}}^\infty \frac{1}{\Omega_1}\left(1 - e^{-\frac{y}{y\rho\psi_E\Omega_2} - \frac{y}{\Omega_1}}\right)dy, \qquad (36)$$

Where $U(x)$ is unit step function as

$$U(x) = \begin{bmatrix} 1, & x > 0 \\ 0, & x < 0 \end{bmatrix}$$

From (35) and (36) we have (34). Substituting (33) and (34) into (32), the CDF of X is thus given by

$$F_X(x) = U\left(\frac{a_2}{a_1} - x\right)\left[1 - e^{-\frac{x}{\psi_I\rho(a_2-a_1x)\Omega_1}}\right.$$

$$\left. + \int_{\frac{x}{\psi_I\rho(a_2-a_1x)}}^\infty \frac{1}{\Omega_1}\left(1 - e^{-\frac{x}{y\rho\psi_E\Omega_2}}\right)e^{-\frac{y}{\Omega_1}}dy\right], (37)$$

By replacing (37) in (21), we can obtain (22).
The proof is completed.

7.3 Appendix 3 - Proof of Remark 1

The proof begins by giving the ergodic rate of D_2 for the high SNR region as follows

$$R_{D_2,PSR}^{HD,\infty} = E\left[\frac{1}{2}\log\left(1 + \min\left(\gamma_{2,D_1}, \gamma_{2,D_2}\right)\right)\right]$$

$$= \frac{1}{2\ln 2}\int_0^\infty \frac{1 - F_X(x)}{1+x}dx, \qquad (38)$$

$$I_5 = \underbrace{\min\left(\frac{a_2}{a_1}, |h_2|^2|h_1|^2\psi_E\rho\right)}_{X}$$

The CDF of X is calculated as follows

$$F_X(x) = \Pr\left(\frac{a_2}{a_1} < |h_2|^2|h_1|^2\psi_E\rho, \frac{a_2}{a_1} < x\right) +$$

$$\Pr\left(\frac{a_2}{a_1} > |h_2|^2|h_1|^2\psi_E\rho, |h_2|^2|h_1|^2\psi_E\rho < y, \frac{a_2}{a_1} > x\right)$$

$$= \Pr\left(\frac{a_2}{a_1} > |h_2|^2|h_1|^2\psi_E\rho, |h_2|^2|h_1|^2\psi_E\rho < y, \frac{a_2}{a_1} > x\right)$$

$$= U\left(\frac{a_2}{a_1} - x\right)\Pr\left(|h_1|^2 < \frac{x}{\psi_E\rho|h_2|^2}, |h_1|^2 < \frac{a_2}{a_1\psi_E\rho|h_2|^2}\right)$$

$$= U\left(\frac{a_2}{a_1} - x\right)\Pr\left(\frac{a_2}{a_1} > x, |h_1|^2 < \frac{x}{\psi_E\rho|h_2|^2}\right) +$$

$$U\left(\frac{a_2}{a_1} - x\right)\Pr\left(\frac{a_2}{a_1} < x, |h_1|^2 < \frac{a_2}{a_1\psi_E\rho|h_2|^2}\right)$$

$$= U\left(\frac{a_2}{a_1} - x\right)\Pr\left(\frac{a_2}{a_1} > x, |h_1|^2 < \frac{x}{\psi_E\rho|h_2|^2}\right)$$

$$= U\left(\frac{a_2}{a_1} - x\right)\int_0^\infty \int_0^{\frac{x}{\psi_E\rho y}} f_{|h_2|^2}(y)f_{|h_1|^2}(z)\,dydz$$

$$= U\left(\frac{a_2}{a_1} - x\right)\int_0^\infty \frac{1}{\Omega_2}\left(1 - e^{-\frac{x}{\psi_E\rho\Omega_1 y}}\right)e^{-\frac{y}{\Omega_2}}dy$$

$$= U\left(\frac{a_2}{a_1} - x\right)\left(1 - 2\sqrt{\frac{x}{\psi_E\rho\Omega_1\Omega_2}}K_1\left(2\sqrt{\frac{x}{\psi_E\rho\Omega_1\Omega_2}}\right)\right), (39)$$

Where $U(x)$ is unit step function as

$$U(x) = \begin{bmatrix} 1, & x > 0 \\ 0, & x < 0 \end{bmatrix}$$

Substituting (39) into (38). We can obtain $R_{D_2,PSR}^{HD,\infty}$.
The proof is completed.

$$F_X(x) = \underbrace{\Pr\left(\frac{\psi_I|h_1|^2 a_2\rho}{\psi_I|h_1|^2 a_1\rho+1} < |h_2|^2|h_1|^2\psi_E\rho, \frac{\psi_I|h_1|^2 a_2\rho}{\psi_I|h_1|^2 a_1\rho+1} < x\right)}_{I_3} + \underbrace{\Pr\left(\frac{\psi_I|h_1|^2 a_2\rho}{\psi_I|h_1|^2 a_1\rho+1} > |h_2|^2|h_1|^2\psi_E\rho, |h_2|^2|h_1|^2\psi_E\rho < x\right)}_{I_4}$$

$$(32)$$

$$I_3 = Pr\left(\frac{\psi_I a_2}{(\psi_I|h_1|^2 a_1\rho+1)\psi_E} < |h_2|^2, |h_1|^2 < \frac{x}{\psi_I\rho(a_2-xa_1)}, \frac{a_2}{a_1} - x > 0\right)$$

$$= U\left(\frac{a_2}{a_1}-x\right) \times \int_0^{\frac{x}{\psi_I\rho(a_2-a_1x)}}\int_{\frac{\psi_I a_2}{(\psi_I y a_1\rho+1)\psi_E}}^{\infty} f_{|h_1|^2}(y) f_{|h_2|^2}(z)\, dy dz$$

$$= U\left(\frac{a_2}{a_1}-x\right) \int_0^{\frac{x}{\psi_I\rho(a_2-a_1x)}} \exp\left(\frac{-\psi_I a_2}{(\psi_I y a_1\rho+1)\psi_E\Omega_2}\right) \frac{1}{\Omega_1}\exp\left(\frac{-y}{\Omega_1}\right) dy$$

$$= U\left(\frac{a_2}{a_1}-x\right) \int_0^{\frac{x}{\psi_I\rho(a_2-a_1x)}} \frac{1}{\Omega_1}e^{-\frac{\psi_I a_2}{(\psi_I y a_1\rho+1)\psi_E\Omega_2}-\frac{y}{\Omega_1}}\, dy$$

$$(33)$$

$$I_4 = \Pr\left(\frac{|h_1|^2\psi_I a_2\rho}{\psi_I|h_1|^2 a_1\rho+1} > |h_2|^2|h_1|^2\psi_E\rho, |h_2|^2|h_1|^2\psi_E\rho < x\right)$$

$$= \Pr\left(|h_2|^2 < \frac{\psi_I a_2}{(\psi_I|h_1|^2 a_1\rho+1)\psi_E}, |h_2|^2 < \frac{x}{|h_1|^2\psi_E\rho}, \frac{a_2}{a_1} - x > 0\right)$$

$$= U\left(\frac{a_2}{a_1}-x\right)\Pr\left(|h_2|^2 < \frac{\psi_I a_2}{(\psi_I|h_1|^2 a_1\rho+1)\psi_E}, |h_2|^2 < \frac{x}{|h_1|^2\psi_E\rho}\right)$$

$$I_4 = U\left(\frac{a_2}{a_1}-x\right) \times \left[\begin{array}{c} \underbrace{\Pr\left(|h_1|^2 < \frac{x}{\psi_I\rho(a_2-xa_1)}, |h_2|^2 < \frac{\psi_I a_2}{(\psi_I|h_1|^2 a_1\rho+1)\psi_E}\right)}_{I_{41}} \\ \underbrace{\Pr\left(|h_1|^2 > \frac{x}{\psi_I\rho(a_2-xa_1)}, |h_2|^2 < \frac{x}{|h_1|^2\psi_E\rho}\right)}_{I_{42}} \end{array}\right]$$

$$(34)$$

$$|h_1|^2\psi_I a_2 < x\psi_I|h_1|^2 a_1 + \frac{x}{\rho} = |h_1|^2 < \frac{x}{\psi_I\rho(a_2-xa_1)}$$

$$I_4 = U\left(\frac{a_2}{a_1}-x\right) \times \left[\underbrace{\Pr\left(|h_1|^2 < \frac{x}{\psi_I\rho(a_2-a_1x)}, |h_2|^2 < \frac{\psi_I a_2}{(\psi_I|h_1|^2 a_1\rho+1)\psi_E}\right)}_{I_{41}} + \right.$$

$$\left. \underbrace{\Pr\left(|h_1|^2 > \frac{x}{\psi_I\rho(a_2-a_1x)}, |h_2|^2 < \frac{x}{|h_1|^2\psi_E\rho}\right)}_{I_{42}}\right]$$